Int. J. Heat Mass Transfer. Vol. 33, No. 1, pp. 69–78, 1990
Printed in Great Britain

0017-9310/90 $3.00+0.00

Measurements of the thermal characteristics of heated offset jets

J. T. HOLLAND and J. A. LIBURDY

Thermal Fluid Sciences Laboratory, Department of Mechanical Engineering, Clemson University, Clemson, SC 29634, U.S.A.

(*Received* 20 *November* 1988 *and in final form* 2 *May* 1989)

Abstract—A study is presented of the thermal characteristics of a turbulent offset jet impinging onto an adiabatic wall. Detailed temperature distributions are used to draw several conclusions concerning the flow characteristics of the jets. Results are also compared with a heated wall jet flow. The three regions studied are the recirculation, impingement and developing wall jet zones. A scaling of the downstream position is presented which collapses much of the thermal details of the jets. However, it is concluded that variation of the flow curvature coupled with entrainment for different offset ratios restrict the scaling. A local similarity of the temperature profiles is substantiated just downstream of impingement.

INTRODUCTION

An offset jet occurs when a discharge of fluid, in the form of a jet, occurs in the proximity of a surface such that the surface influences the entrainment characteristics asymmetrically about the jet centerline. The most obvious effect is the deflection of the jet towards the wall and eventual impingement onto the surface. There are many situations in which this type of flow geometry occurs such as flows entering into heat exchangers, discharge of power plant effluents, and flows into combustion chambers. In this paper the flow geometry under consideration is a two-dimensional turbulent jet with the nozzle discharge a variable distance above a flat surface, as shown in Fig. 1. In all cases studied the jet discharge direction and the surface are horizontal. The goal is to determine the jet downstream thermal characteristics when the surface is adiabatic. The jet can be divided into the three flow regimes shown in Fig. 1, the recirculation region, the impingement region, and the wall jet region.

The details of the flow have been studied by several authors. The first detailed studies of the mean flow characteristics were by Bourque and Newman [1]. They presented an analysis of the mean flow characteristics which predicted the location of impingement as a function of offset ratio (the ratio of the distance from the jet exit to the impingement surface and the jet nozzle diameter). Pelfrey and Liburdy [2] in a more recent study provided details of the mean and turbulent flow characteristics. They showed how the entrainment, local pressure and turbulent energy components were influenced by the jet curvature prior to impingement. A detailed literature review of the fluid mechanics aspects of the offset jet is provided by Pelfrey [3].

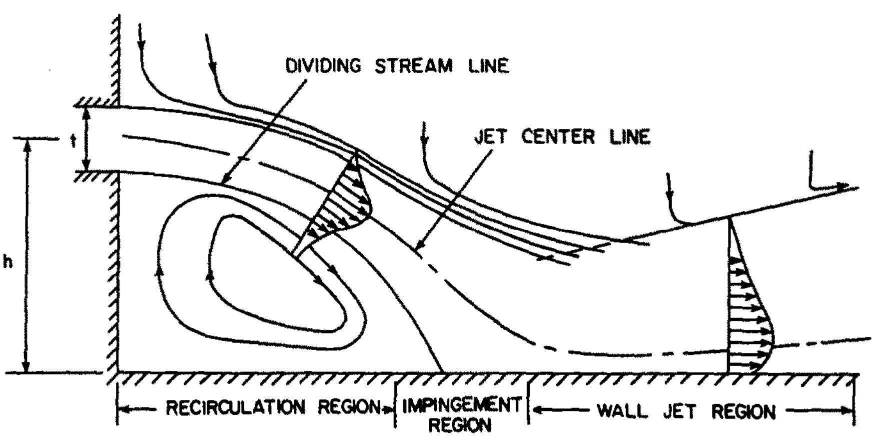

Fig. 1. Flow geometry.

Very little is available in the literature concerning the thermal and heat transfer characteristics of offset jets. There are several studies of the heat transfer of impinging jets. One of the earliest works is by Perry [4] who investigated the effect of changing the impingement surface orientation relative to the jet flow direction. Gardon and Akfirat [5] measured the local heat transfer coefficients on a heated surface normal to an impinging turbulent jet. They investigated the effects of nozzle size, jet flow rate, and nozzle-to-plate spacing. Gardon and Akfirat [6] also studied the effects of increased turbulence intensity on the increase of the local heat transfer rates at the surface. Striegl and Diller [7] measured the effect of entrainment temperature on the local heat transfer rates for impinging jets.

A similar type of flow geometry, the flow over a backstep, has recently been studied quite extensively, primarily in terms of its fluid flow characteristics. Aung and Goldstein [8] experimentally studied flow over a heated backstep. They obtained information of the temperature distribution using a Mach–Zender interferometer for the case of a uniformly heated wall. They measured a maximum heat transfer rate at the impingement region. Several numerical predictions have been made for this flow. Aung [9] reviewed both the laminar and turbulent cases.

In a more recent study predictions of the unheated turbulent case were presented by Raghunath and Liburdy [10] using modified forms of the k–ε turbulence model to account for flow curvature and wall interactions. The heated offset jet impinging onto a cold isothermal wall is numerically modelled by Raghunath *et al.* [11]. The turbulence models used in these predictions are inadequate. It is suspected that this is due to the strong influence of curvature strain rate as discussed by Pelfrey and Liburdy [12].

To the authors' knowledge the only other investigation of a non-isothermal offset jet is the analytical and experimental study by Hoch and Jiji [13]. They measured the temperature distribution in a two-dimensional jet offset from an adiabatic surface. They found the temperature within the recirculation region to be essentially uniform and to decrease with increasing offset ratio. Consistently, the jet temperature decay rate increases with increasing offset ratio.

This paper examines the thermal characteristics of heated offset jets where the impinging surface is adiabatic. The offset ratio is defined as the vertical distance from the center of the nozzle to the impinging surface divided by the nozzle thickness. The effects of offset ratio and jet exit Grashof number are presented. The Grashof number is based on the jet exit temperature minus the ambient temperature, the nozzle thickness, and all fluid properties evaluated at the jet exit temperature. The range of test conditions are listed in Table 1. All experiments were run at a single Reynolds number of 15 000 based on the exit velocity and nozzle thickness. This assured a fully turbulent flow. It has been shown by Bourque and Newman [1], Sawyer [14], Parameswaran and Alpay [15] and others that once the flow is turbulent there is no discernible Reynolds number effect on the impingement location or other mean flow characteristics. Of interest here is the thermal energy decay of the jet, the energy distribution within the recirculation region, and downstream redevelopment of the wall jet after impingement. Since the surface is adiabatic the thermal energy distribution is a result of the entrainment characteristics of the jet with its surroundings.

Table 1. Test conditions

Offset ratio	Grashof number	Exit temperature (°C)	Ambient temperature (°C)
3	411	67	24
3	477	90	25
3	494	112	24
7	411	68	24
7	477	91	24
7	494	112	25
11	411	67	24
11	477	89	25
11	494	112	25
0	411	67	24
0	477	89	25
0	494	112	26

EXPERIMENTAL APPARATUS AND PROCEDURES

A two-dimensional jet of heated air was discharged above an offset adiabatic surface. A schematic of the apparatus is shown in Fig. 2. Air was supplied by a compressor to a series of two pressure regulated surge tanks which elimated any variations in the flow rate. The flow rate was controlled with two valves upstream of a laminar flow element used to measure the volumetric flow rate. The measured flow rate was corrected for temperature and pressure. The air was heated with a series of electrical resistance heaters. Both heaters were regulated using variable resistance controllers. The flow then passed through a low aspect ratio diffuser, a series of screens, and then entered a plenum chamber. A two-dimensional nozzle (7.62 cm wide by 0.5 cm high, approximately 15 : 1 aspect ratio) directed the flow horizontally into the ambient air which was nominally at 25°C. The nozzle was designed based on an ASME specification with an elliptical contour on the upstream side of the nozzle and a discharge coefficient of 0.89. Two sidewalls of plexiglass were used to maintain the two-dimensionality of the flow. The sidewalls extended well downstream of the nozzle exit and the impingement location. The two-dimensionality at the nozzle was checked by measuring the exit velocity and temperature across the span of flow. The velocity was measured with a pitot tube and was uniform to within 0.7% out to 3.2 cm on either side of

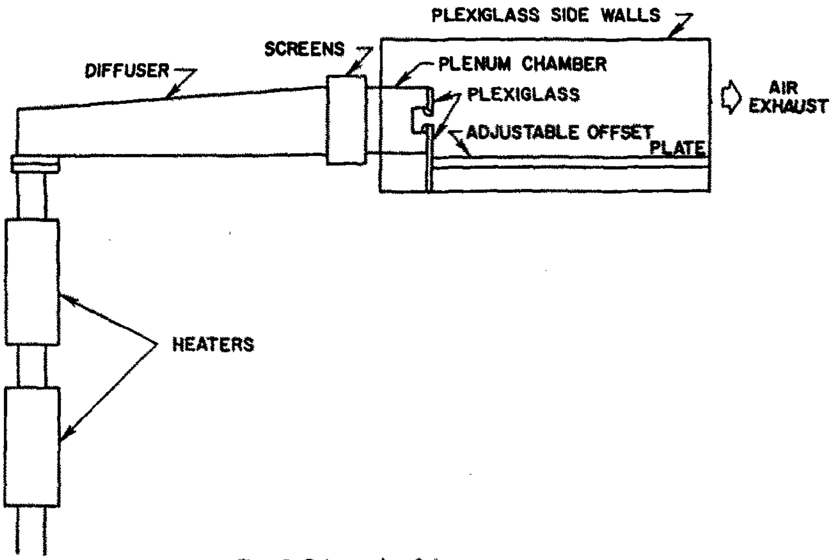

FIG. 2. Schematic of the test apparatus.

the jet centerline. The spanwise variation of temperature was checked at the nozzle exit and several downstream locations to within 2 mm of the sidewalls. The temperature did not vary across the flow by more than 1% of the temperature difference between the jet exit and the ambient.

The offset surface was constructed from 7.62 cm wide, 30.48 cm long, and 0.635 cm thick balsa wood chosen for its low thermal conductivity. The underside of the surface was packed with 4 in. of fiberglass insulation. Thermocouples (0.25 mm diameter wire) were embedded in the underside of the wood to within 1.6 mm of the surface. These thermocouples were placed at 6.35 mm increments beginning at the exit plane of the jet up to 7.62 cm along the surface and then at 12.7 mm increments for the next 7.62 cm and finally two additional thermocouples were located at 20.32 and 25.4 cm from the exit of the jet. This positioning allowed the wall temperature to be measured with high spacial resolution in the recirculation and impingement regions for all offset ratios studied.

The jet exit temperature was determined using a thermocouple placed in the center of the plenum chamber. The temperature in the flow field was measured with a very fine wire thermocouple probe. The probe was constructed from 0.0254 mm chromel and alumel wire which was strung across two 0.4 mm diameter supports that matched the thermocouple material. The wires were positioned such that the sensor bead (approximately 0.07 mm) was midway between the 0.5 cm distance between the two supports. The support wires extended back 0.62 cm where they entered into brass tubing which formed the main probe support structure. The support structure was slightly bent such that the sensor could be positioned upstream of the probe support. Since the lead wires of the probe extended away from the sensor, across the flow, the conduction errors were reduced. The convection and radiation errors were calculated to be less than 0.5°C at 45 m s^{-1} which is well beyond the velocities encountered in this study. The sensor was calibrated against a resistance temperature detector. A total uncertainty of the measured temperature was calculated to be 0.7°C. The probe was mounted on a two-dimensional traversing system with a 0.05 mm resolution. The sensor signal was monitored using a PDP 11/03 computer with a preamplifier and A/D converter. The temperature was sampled at 200 Hz using a total of 1023 data points per sample. (Other sampling rates were tested to assure that the signal was stationary.)

The entire jet facility was housed in an environmentally controlled room. The ambient temperature was monitored before and after each experimental run. The ambient temperature used to reference the jet exit temperature was the average of the temperatures measured at three locations above the flow. These were above the jet exit, above the impingement region, and above the wall jet region. The temperature variation among these three locations was less than 1°C.

Each experiment was run after reaching a steady state as indicated by the temperatures of the offset surface (this took approximately 45–60 min). The temperature distribution within the flow was measured by traversing the sensor vertically at nine or more locations along the surface. Five profiles were taken within the recirculation region and at least four downstream of impingement. After each vertical traverse the ambient temperature was recorded and checked to assure that it did not drift during the run.

The temperature, T, is presented in non-dimensional form as θ defined below, where T_{inf} is the ambient temperature and T_{ex} the jet exit temperature

$$\theta = (T - T_{inf})/(T_{ex} - T_{inf}). \quad (1)$$

In this way the maximum value of θ occurs at the jet exit and decreases to zero in the ambient surroundings. The downstream variation of θ represents the loss of the jet's original thermal energy which, for the adiabatic wall condition is solely due to the entrainment process. In addition, the temperature distributions in the wall jet region are normalized as θ/θ_w where θ_w is the non-dimensional temperature of equation (1) with T replaced by the wall temperature which is the maximum temperature in a given cross section of the flow

$$\theta_w = (T_{wall} - T_{inf})/(T_{ex} - T_{inf}).$$

RESULTS AND DISCUSSION

Prior to measuring the thermal characteristics of the offset jet the unheated flow field was examined to assure that it was consistent with others reported in the literature. The impingement location was checked for each of the offset ratios. This was done by inserting a long rod into the flow which had a very fine thread, approximately 1.9 cm long, attached to its tip. The rod was placed such that the thread was positioned approximately 1 mm above the surface. The rod was then moved along the surface such that the thread waved in the direction of the flow. The impingement location was identified as the location on the surface where the thread just changed flow direction, from upstream to downstream, or vice versa depending on the traversing direction of the rod. The tests were repeated with the rod slowly traversing in both the upstream and downstream directions. When the rod was moving in the upstream direction the impingement location appeared to be slightly further downstream than when the rod was traversing in the downstream direction. The average values of the impingement locations are given in Table 2 and are compared to those reported by Sawyer [14] for each offset ratio. The values for this study are approximately 3, 8 and 9% different from those of Sawyer [14]. The impingement location was also measured for the heated jet. At the highest exit temperature the impingement location was measured and found to be indistinguishable from the unheated case for the same offset ratio. This result suggests that, for the temperatures studied, the buoyancy effects on the mean flow are negligible.

It has been shown by Sawyer [14] and Bourque and Newman [1] that the impingement distance per nozzle thickness is uniquely determined by the offset ratio.

Table 2. Impingement locations

Offset ratio	x (cm)	Sawyer [14] x (cm)	x/t	I_r
3	3.53	3.43	7.02	1.77
7	6.25	6.85	12.42	1.00
11	8.59	9.50	17.07	0.73

With this in mind the results of this study have been scaled by the impingement distance for an offset ratio of 7 divided by the impingement distance of the case being examined. The choice of 7 is arbitrary. This scaling forces all of the impingement locations to coincide. The ratios of the impingement distances are given in Table 2 as I_r. This scaling is used to represent the temperature variation away from the jet exit in the horizontal, x, direction by using the scaled variable $x' = xI_r$.

In order to nondimensionalize the temperature distributions in terms of θ the local surface temperature must be known. The temperatures recorded by the thermocouples embedded in the wall were slightly below the recorded values of the probe just above (0.5 mm) the wall for all locations along the wall. It is felt that this difference was because the embedded thermocouples were too far from the surface to accurately measure the surface temperature, this is a result of the low thermal conductivity of the wall material. Since we are approximating an adiabatic condition such that the temperature gradient in the air at the surface is zero, it was decided to use the temperature measured by the probe 0.5 mm away from the wall surface to represent the wall temperature. The results presented here would not be detectably altered if an average temperature between the wall and probe temperature had been used to represent the surface temperature.

The variation of the surface temperature along the wall is shown in Fig. 3 for the wall jet and for three offset ratios, 3, 7, and 11, where an offset ratio of 0 represents the wall jet. The use of x'/t, where t is the nozzle thickness, as the downstream coordinate collapses all of the impingement locations at 12.42. (Obviously the wall jet does not have an impingement location and for this case the temperature is plotted vs actual distance x normalized by t.) For each of the offset jets the surface temperature has a peak within the recirculation region. This same trend was detected by Hoch and Jiji [13] for an offset ratio of 8.7. Our results indicate that the peak temperature occurs closer to the jet exit for larger offset ratios. The peak temperature for an offset ratio of 3 occurs very close to the impingement location. The ratio of the maximum non-dimensional surface temperature in the recirculation region to the non-dimensional impingement temperature increases with increasing offset ratio. This ratio is 1.0, 1.04, and 1.12 for offset ratios of 3, 7, and 11, respectively.

The characteristics of the temperature distribution can be related to the wall pressure. The wall pressure was measured by Pelfrey and Liburdy [2] for an offset ratio of 7. They found that there is a wall pressure minimum and a corresponding increased velocity just above the wall located at approximately $x'/t = 6.5$. This location compares well with the local surface temperature peak in this study for an offset ratio of 7. It is interesting that for large offset ratios the wall region of the recirculation zone apparently experi-

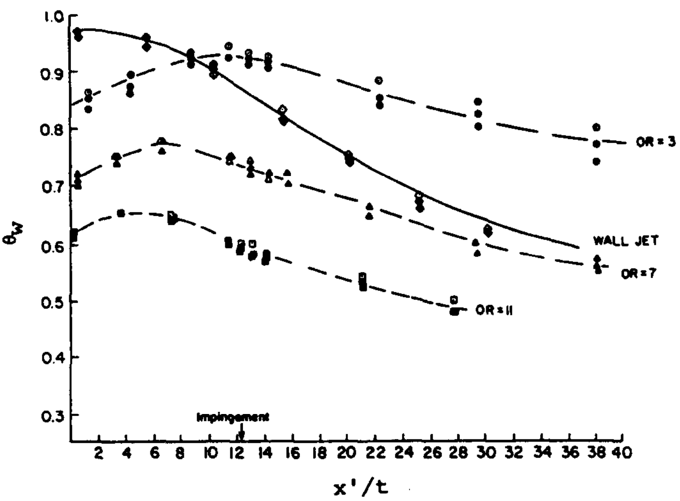

FIG. 3. Surface temperature distribution θ_w; OR is the offset ratio.

ences flow acceleration and increasing surface temperature far removed from impingement. The variation of the wall characteristics for different offset ratios suggests that the details of the recirculation region do not scale with the impingement distance.

The large reduction of the surface temperature with increased offset ratio, shown in Fig. 3, suggests that the jet energy decay rate prior to impingement is substantially larger for larger offset ratios. This is an indication that the entrainment cooling increases with increasing offset ratio. The results of Pelfrey and Liburdy [2] show an increased entrainment rate of the offset jet relative to the wall jet and that the entrainment rate correlates with a large increase in curvature strain rate. Noting the variation of the temperature decay rates for the different offset ratios it is reasonable to conclude, then, that the curvature strain rate increases with increased offset ratio. This suggests that for large offset ratios the flow experiences large curvature much closer to the impingement location. This is consistent with the inability to scale the surface temperature distribution with the impingement distance.

Detailed temperature profiles within the recirculation region are shown in Figs. 4(a) and (b) and near the impingement location in Fig. 5. A comparison of Figs. 4(a) and (b) shows that there are very small downstream temperature variations within the recirculation region for each of the offset ratios. At the lower value of the offset ratio the relative thermal energy content is higher and the vertical temperature distribution is essentially uniform up to the lower side of the jet (near what is called the dividing streamline). Also, for the low offset ratios, the temperature in the recirculation region is nearly identical to the temperature in the main jet.

The maximum temperature decay of the jet prior to impingement is shown in Fig. 6, where θ_{max} is defined as $(T_{max}-T_{inf})/(T_{ex}-T_{inf})$ where T_{max} is the maximum jet temperature at a given downstream cross section of the jet. For larger offset ratios the temperature decay rate increases. This is consistent with the previous conclusion based on the lower temperatures within the recirculation region for larger offset ratios caused by increased entrainment. For an offset ratio of 3 the decay rate is virtually identical to that of the wall jet.

The temperature decay rate for normally impinging jets has been reported by Striegl and Diller [16] and the effects of thermal entrainment is presented by them in ref. [17]. The temperature was scaled in the form

$$\theta_c = (T_c - T_{inf})/(T_{ex} - T_{inf})$$

where T_c is the jet centerline temperature. The decay of θ_c was found to correlate well as $\theta_c = C_1(x/t_o)^{-1/2}$, where C_1 is a constant and t_o is defined as $C_2 t$ where C_2 is the nozzle discharge coefficient. Based on their results, using the correlation of their heat transfer data, not direct temperature measurements, the value of C_1 is 2.13. An attempt to curve fit $\theta_{j,max}$ in the same form as θ_c was unsuccessful for either of the normalized downstream distances x/t or x'/t. This difference of scaling and decay rate with normally impinging jets is most likely due to the jet flow curvature prior to impingement. This can be shown in the plot of θ_{max} vs $(x'/t_o)^{-1/2}$ in Fig. 7. Note that the independent variable, $(x'/t_o)^{-1/2}$, decreases in the downstream direction. The larger offset ratio jets experience a more rapid temperature decrease prior to impingement.

The non-dimensional temperature profiles, θ, for the entire flow region are shown in Figs. 8(a)–(d) for the wall jet and each offset ratio. Note that the horizontal and vertical axes are scaled differently. The vertical distance from the plate, y, is scaled by the distance from the surface to the center of the nozzle,

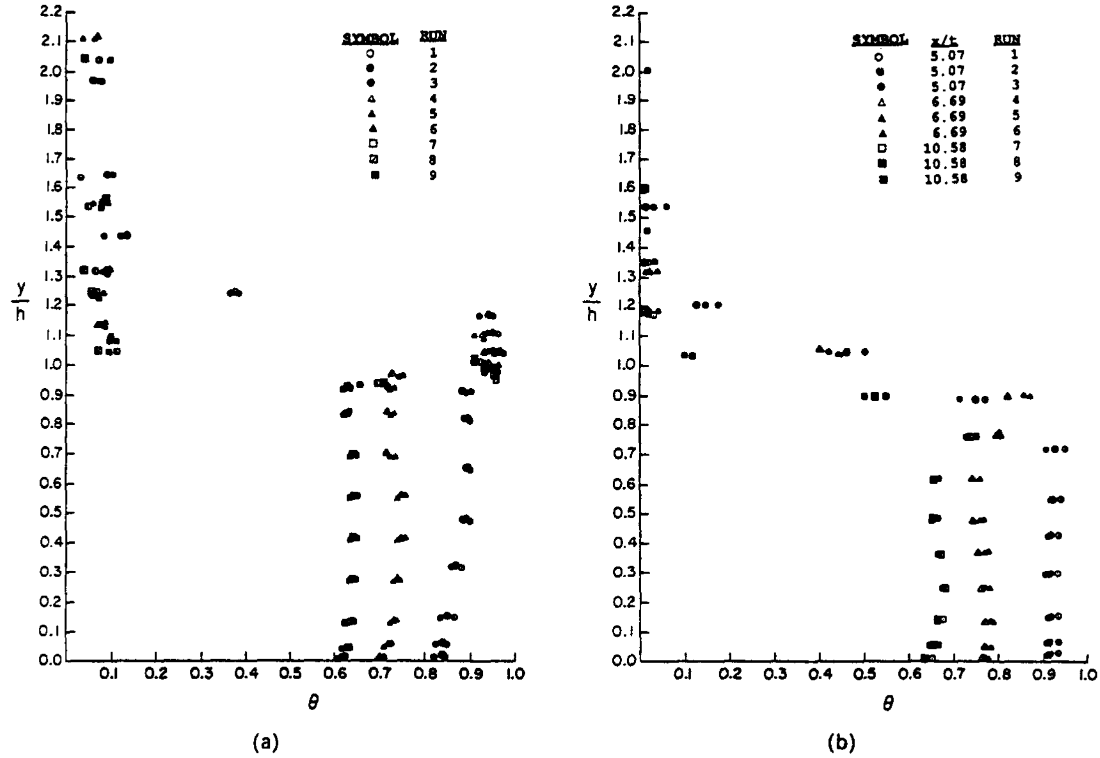

FIG. 4. Temperature profiles in the recirculation region: (a) 3 mm from the jet exit; (b) midway in the recirculation region.

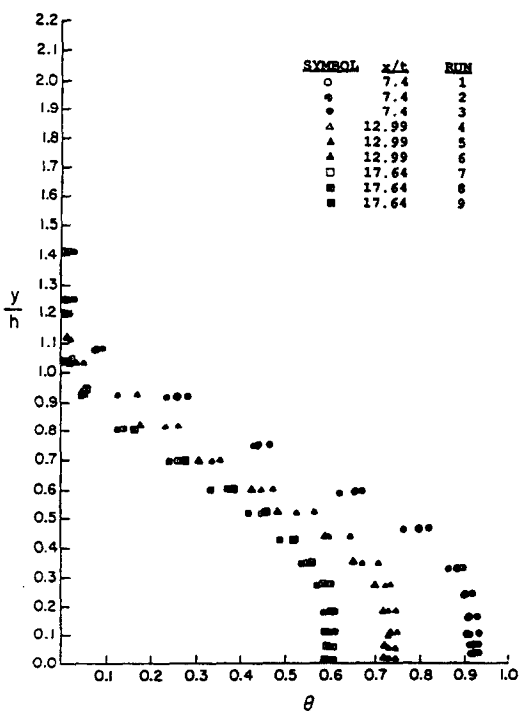

FIG. 5. Temperature profiles in the impingement region.

h. The temperature scale is at the top of each figure with each vertical traverse scaled from zero to one as indicated. At each downstream location for a given offset ratio the non-dimensional temperatures collapse onto a single curve for all three exit temperatures studied. The temperature scaling is therefore appropriate for a single geometry but does not necessarily extend uniformly to different offset ratios.

The thermal decay characteristics of the offset jet downstream of impingement are presented in terms of the jet temperature half-width measured by the thermal boundary layer thickness. The temperature half width, $\delta_{T1/2}$, is defined as the distance above the surface where the value of θ is one-half of the maximum value of θ. In the wall jet region the maximum temperature occurs at the surface. The location of the temperature half width was determined, when necessary, by linear interpolation between data of the measured temperature profiles.

The downstream variation of the temperature half width is shown in Fig. 9. Results are shown for all offset ratios and for all jet exit temperatures. Both the jet half width, $\delta_{T1/2}$, and the normalized downstream distance, x/t, are scaled by the relative downstream distance to impingement l_r. The results are fairly well

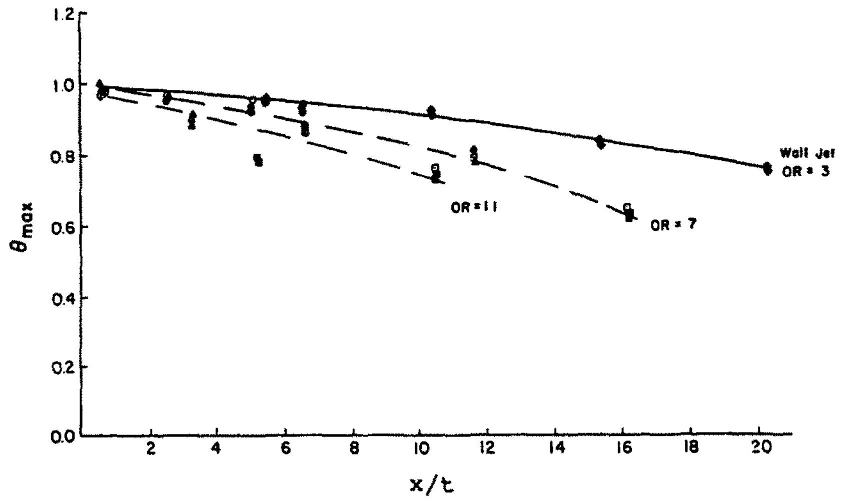

FIG. 6. Decay of the maximum jet temperature in the recirculation region.

correlated except for somewhat larger thickness values downstream for the offset ratio of 11. A minimum half width occurs between $x'/t = 18$ and 21 which is between 6 and 9 nozzle thicknesses downstream of impingement. The growth rate for the wall jet is based on x/t since I_r is undefined for this case. The slopes of the offset jets downstream of impingement and the wall jet are very close. Based on these data the jet thickness can be correlated fairly well when scaled with I_r. The differences that are seen for the larger offset ratio may be attributed to the suspected smaller radius of curvature of the jet as it approaches the surface compared to that of the smaller offset ratio cases. However, it is recommended that the impingement location be measured more precisely before a quantitative evaluation is made.

Downstream of impingement the cross stream temperature distribution is found to be well represented by a single function when the cross stream coordinate is scaled by the temperature half width and θ is scaled by θ_{max}. Figure 10 shows the temperature profiles in the developing wall jet region. The curve fitted data of Hoch and Jiji [13] for one offset ratio are also shown. Not all of the data are shown on the figure, however, a least squares curve fit was performed using all of the data from this study. The correlation was required to match the wall boundary value, $\theta = \theta_{max}$, all the data are within $\pm 5\%$ of the correlation

$$\theta/\theta_{max} = \exp[(-0.804y/\delta_{T1/2})^2]. \quad (2)$$

This correlation differs from the profile given by Hoch and Jiji [13] in that they used the velocity half width, $y_{1/2}$, rather than the temperature half width, $\delta_{T1/2}$, to normalize the distance from the surface, y. Their results indicate a coefficient in the exponential term of 0.833 rather than 0.804.

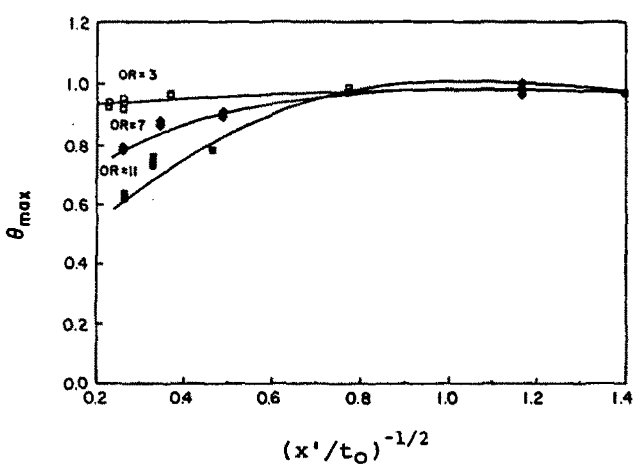

FIG. 7. Decay of the maximum jet temperature using the free jet scaling coordinate.

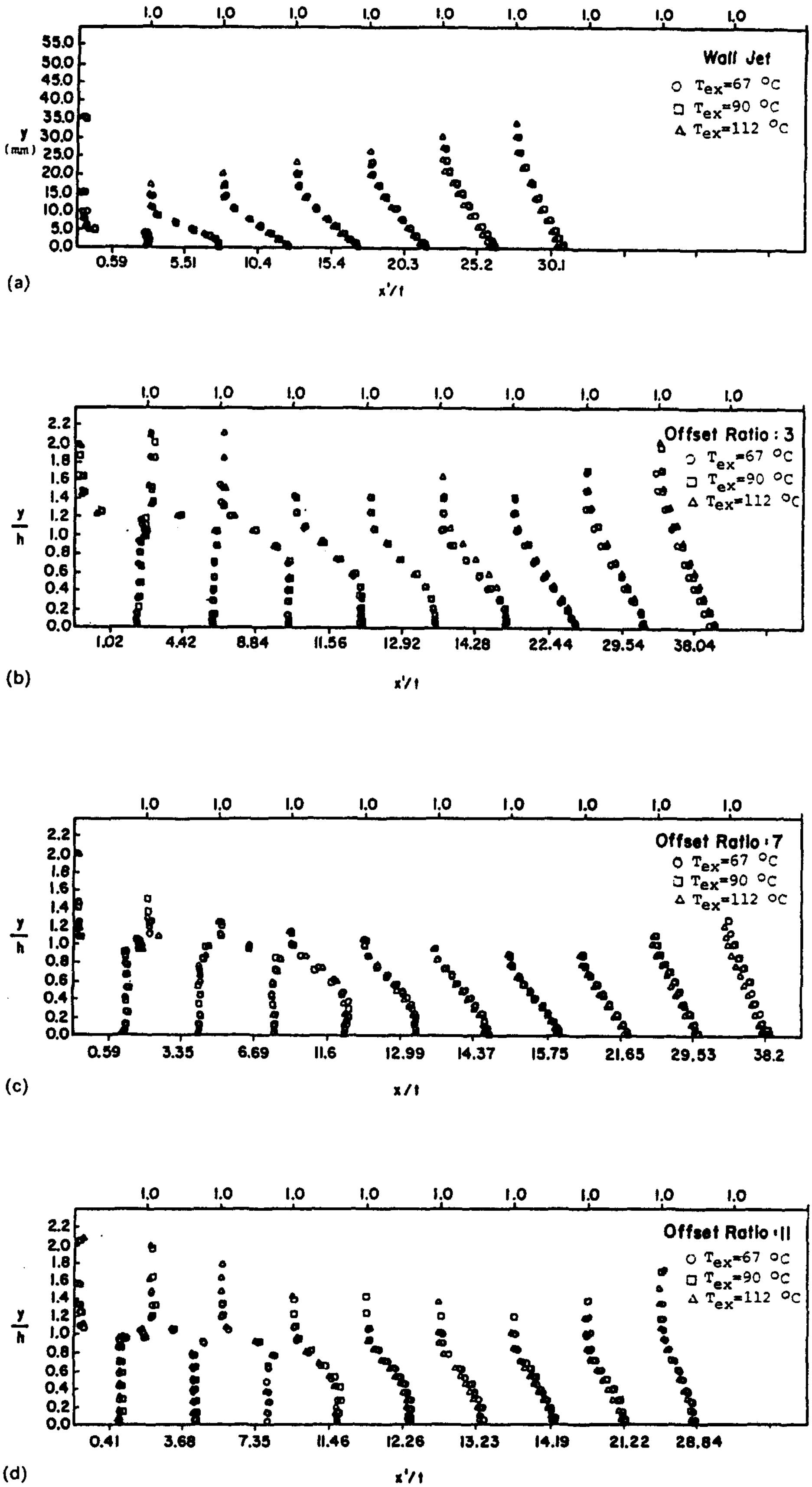

FIG. 8. Temperature profiles for all cases of offset ratios and temperatures: (a) wall jet; (b) offset ratio of 3; (c) offset ratio of 7; (d) offset ratio of 11.

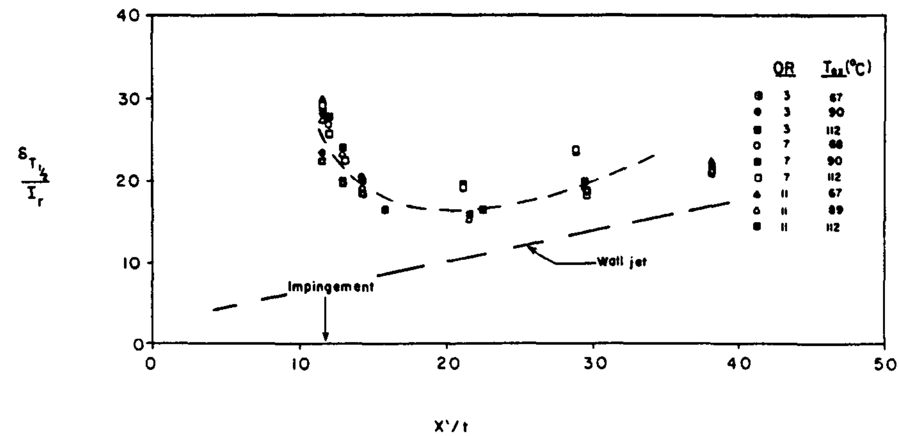

FIG. 9. Spread of the jet downstream of impingement where the jet half width is scaled with the impingement distance parameter I_r.

CONCLUSIONS

Detailed temperature measurements of heated offset jets at three different offset ratios are presented. Results are also compared with the measurements of a wall jet. The impinging surface was adiabatic such that the downstream thermal characteristics illustrate the entrainment characteristics of the flow. The following conclusions can be made based on the data presented. The thermal energy content within the recirculation region remains relatively uniform for both low and high offset ratio jets. The temperature within the recirculation region is close to the impingement location temperature, however there is evidence that the thermal distribution is dependent on the offset ratio, especially near the wall. Based on the measured temperature decay rates and the correlation of decay rate and entrainment and correlation of entrainment and mean flow strain rate due to curvature it is surmised that high offset ratio jets experience greater flow curvature and entrainment of ambient fluid. There is evidence that just downstream of impingement the temperature profiles become locally similar based on the wall temperature and jet half width scaled with the impingement distance.

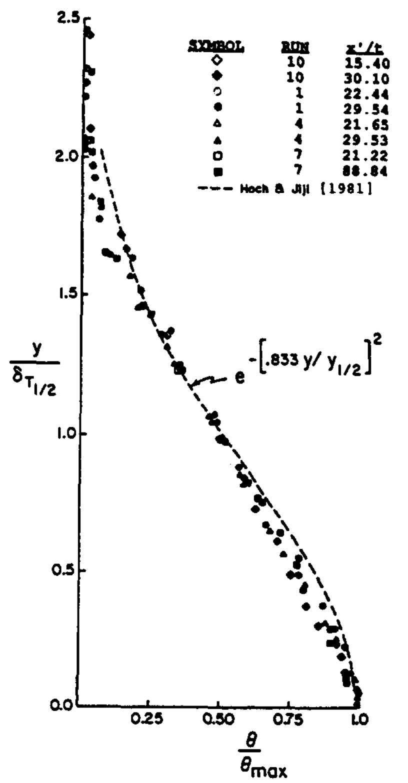

FIG. 10. Non-dimensional temperature profile downstream of impingement.

REFERENCES

1. C. Bourque and B. G. Newman, Reattachment of a two dimensional incompressible jet to an adjacent plate, *Aeronaut. Q.* **11**, 201–232 (1960).
2. J. R. R. Pelfrey and J. A. Liburdy, Mean flow characteristics of a turbulent offset jet, *J. Fluids Engr* **108**, 82–88 (1986).
3. J. R. R. Pelfrey, Characteristics of a turbulent plane offset jet, Ph.D. Dissertation, Clemson University, Clemson, South Carolina (1984).
4. K. P. Perry, Heat transfer by convection from a hot gas jet to a plane surface, *Proc. Inst. Engrs* **186**, 775–784 (1953).
5. R. Gardon and J. C. Akfirat, Heat transfer characteristics of impinging two-dimensional air jets, *J. Heat Transfer* **9**, 101–108 (1966).
6. R. Gardon and J. C. Akfirat, The role of turbulence in determining the heat transfer characteristics of impinging jets, *Int. J. Heat Mass Transfer* **8**, 1261–1272 (1965).
7. S. A. Striegl and T. E. Diller, The effect of entrainment temperature on jet impingement heat transfer, *J. Heat Transfer* **106**, 27–33 (1984).
8. W. Aung and R. J. Goldstein, Heat transfer of turbulent heated flow downstream of a rearward facing step, *Israel J. Technol.* **10**, 35–41 (1972).
9. W. Aung, Separated forced convection, *ASME–JSME*

Thermal Engng Joint Conf. Proc., Honolulu, Hawaii, 20–24 March, Vol. 2, pp. 499–515 (1983).
10. R. Raghunath and J. A. Liburdy, Predictions of a turbulent offset jet, AIAA/ASME 4th Fluid Mechanics, Plasma Dynamics, and Laser Conf., Atlanta, Georgia, 12–14 May (1986).
11. G. Raghunath, R. Kumar and J. A. Liburdy, Application of a k–ε closure to a heated turbulent offset jet, *Proc. Eighth Int. Heat Transfer Conf.*, San Francisco, California, 17–22 August (1986).
12. J. R. R. Pelfrey and J. A. Liburdy, Effects of curvature on the turbulence of a two-dimensional jet, *Exp. Fluids* **4**, 143–149 (1986).
13. J. Hoch and L. M. Jiji, Theoretical and experimental temperature distribution in two dimensional turbulent jet–boundary interaction, *J. Heat Transfer* **103**, 331–335 (1981).
14. R. A. Sawyer, The flow due to a two-dimensional jet issuing parallel to a flat plate, *J. Fluid Mech.* **9**, 543–560 (1960).
15. V. Parameswaran and S. A. Alpay, Studies on re-attaching wall jets, *Trans. Can. Soc. Mech. Engrs* **3**, 83–89 (1975).
16. S. A. Striegl and T. E. Diller, An analysis of the effect of entrainment temperature on jet impingement heat transfer, *J. Heat Transfer* **106**, 804–810 (1984).

MESURE DES CARACTERISTIQUES THERMIQUES DE JETS CHAUDS IMPACTANTS

Résumé—On présente une étude des caractéristiques thermiques d'un jet turbulent qui frappe une paroi adiabatique. Des distributions détaillées de température sont utilisées pour tirer quelques conclusions concernant les caractéristiques d'écoulement du jet. Les résultats sont comparés avec le cas d'une paroi chauffée. Les trois régions étudiées sont les zones de recirculation, d'impact et de développement sur la paroi. On présente une mise en échelle qui fait disparaître la plupart des détails thermiques des jets. Néanmoins on conclut que la variation de la courbure de l'écoulement couplée avec l'entraînement pour différentes conditions restreint la mise en échelle. Une similitude locale des profils de température est réalisée juste sous l'impact.

MESSUNG DES THERMISCHEN VERHALTENS EINES BEHEIZTEN STRAHLS

Zusammenfassung—Es wird das thermische Verhalten eines turbulenten Strahls untersucht, der auf eine adiabate Wand aufprallt. Dabei werden detaillierte Temperaturverteilungen benutzt, um verschiedene Folgerungen für die Strömungscharakteristik des Strahls zu ziehen. Die Ergebnisse der Untersuchungen werden mit der Strahlströmung an einer beheizten Wand verglichen. Die betrachteten Regionen sind das Rückströmungsgebiet, die Auftreffregion und die sich ergebende Wandströmung. Es wird eine Skalierung der stromabwärtigen Position vorgestellt, die wesentliche thermische Details des Strahls enthält. Trotzdem ergibt sich die Schlußfolgerung, daß die Änderung der Strahlkrümmung zusammen mit dem Entrainment bei unterschiedlichen Abstandsverhältnissen die Anwendbarkeit der Skalierung beschränkt. Es ergibt sich eine lokale Ähnlichkeit des Temperaturprofils etwas unterhalb des Aufprallpunktes.

ИЗМЕРЕНИЯ ТЕПЛОВЫХ ХАРАКТЕРИСТИК НАГРЕТЫХ СТРУЙ, РАЗВОРАЧИВАЮЩИХСЯ ПРИ СОУДАРЕНИИ СО СТЕНКОЙ

Аннотация—Исследуются тепловые характеристики турбулентной струи, ударяющейся об адиабатическую стенку. Для некоторых заключений о характеристиках течения струй используются детальные распределения температур. Результаты сравниваются с данными для течения нагретой пристенной струи. Изучаются три области: область рециркуляции, соударения и развивающейся притенной струи. Определен характерный масштаб размеров струи вниз по течению, на котором еще сказывается большая часть тепловых характеристик струй. Однако сделан вывод о том, что изменение изгиба струи, зависящее от ее импульса, ограничивает применимость определенного выше масштаба. Обосновано локальное подобие температурных профилей непосредственно вниз по течнию от места соударения.